On the Absorption Cross Section of CdSe Nanocrystal Quantum Dots

C. A. Leatherdale, W.-K. Woo, F. V. Mikulec, and M. G. Bawendi*

Massachusetts Institute of Technology, 77 Massachusetts Avenue, Cambridge, Massachusetts 02139

Received: February 27, 2002; In Final Form: May 6, 2002

The linear absorption cross section is a crucial parameter to the design of nanocrystal quantum dot devices and to the interpretation of spectroscopic data. We measure and report the size-dependent absorption cross section of CdSe nanocrystal quantum dots. We compare the results for absorption far above the band edge, where the quantum dot density of states may be approximated as a continuum, to simple theoretical models of light scattering from light-absorbing small particles. Excellent agreement with theory is found for dilute dispersions in hexane. We find that for absorption at 350 nm the per particle absorption cross section C_{abs} (in cm^2) for CdSe is $C_{abs} = (5.501 \times 10^5)a^3\ cm^{-1}$, where a is the particle radius in cm. The absorption cross section is observed to be largely insensitive to the solvent refractive index. Detailed modeling of the effect of the ligand shell may be necessary to understand the lack of sensitivity of the absorption properties of nanocrystal quantum dots to the refractive index of the medium.

I. Introduction

Semiconductor quantum dots (QDs) are the subject of intense research for their size-dependent optoelectronic properties,[1−3] application in novel linear and nonlinear optical devices,[4] and use as biological tags.[5−7] For the design of such devices, as well in detailed studies of the dynamics of quantum-confined electrons and holes, knowledge of the QD absorption cross section is essential. Surprisingly, the absolute linear absorption cross section for interband transitions in CdSe QDs is not well-known. One reason for the absence of such a key parameter may be the difficulty of accurately counting particles rather than ions or molecules. To date, all published determinations of QD absorption cross sections have relied either on decomposing the nanoparticle and analyzing for the concentration of one of the component ions[8−10] or on gravimetric analysis.[11] Both procedures require narrow size distributions to avoid large uncertainties in the particle concentration and thus the extinction coefficient. In gravimetric methods, the mass of the surface ligands adds further uncertainty. In this report, nearly monodisperse dispersions of CdSe are used to determine the absorption cross section on the basis of measured reaction yields.

Available theoretical models for the QD absorption cross section range from simple light-scattering models[12−15] based on the polarizability of dielectric spheres to more complex calculations[16−20] aimed at accounting for the self-reaction of the QD in the light field. In all cases, the degree of polarization and thus the absorption cross section depends on the refractive index contrast inside and outside the QD. We show here that simple theory is in excellent agreement with experiment for dilute solutions of QDs in hexane. Our experiments indicate that the absorption cross section is largely independent of solvent refractive index. The low permittivity ligand shell may reduce the sensitivity of the QD absorption cross section to the refractive index of the medium.

II. Theory

For optical transitions far from any strong resonances and far from the band edge where the QD density of states may be approximated as a continuum, the QD absorption cross section may be modeled by using the formalisms from the light scattering of small particles.[21] The extinction cross section is the sum of the absorption (C_{abs}) and scattering cross sections (C_{scat}):

$$C_{ex} = C_{abs} + C_{scat} \tag{1}$$

Light, as it propagates a distance l through a medium with a refractive index m_3 containing N particles per unit volume, is reduced in intensity by $e^{-C_{ex}Nl}$. For particles in which the radius (a) is much smaller than the wavelength in the medium (λ/m_3), C_{abs} is much greater than the C_{scat}, and scattering can be neglected. For absorbing particles with isotropic polarizability, C_{abs} is given by

$$C_{abs} = 4\pi k \mathrm{Re}(i\alpha) = \frac{8\pi^2 m_3}{\lambda}\mathrm{Re}(i\alpha) \tag{2}$$

where λ is the wavelength in vacuum and α is the polarizability of the particle. The polarizability of dielectric spheres with radius a is given by

$$\alpha = \frac{m_1^2 - m_3^2}{m_1^2 + 2m_3^2}a^3 \tag{3}$$

where $m_1 = n_1 - ik_1$ is the complex refractive index of the particle. An alternative expression that is useful for further calculations and is identically equal to eqs 2 and 3 when the volume fraction of particles is much less than 1 was derived by Ricard et al:[16]

$$C_{abs} = \frac{\omega}{m_3 c}|f(\omega)|^2 2n_1k_1\left(\frac{4}{3}\pi a^3\right) \tag{4a}$$

$$f(\omega) = \frac{3m_3^2}{m_1^2 + 2m_3^2} \tag{4b}$$

Written in this manner, C_{abs} is proportional to the product of the "bulk" absorption coefficient ($2n_1k_1$) and a local field factor

* Corresponding author. E-mail: mgb@mit.edu.

10.1021/jp025698c CCC: $22.00
Published on Web 07/16/2002

that is equal to the ratio of the applied electric field to the electric field inside the sphere.

III. Experimental Section

CdSe colloidal QDs capped with trioctylphosphine oxide (TOPO)/trioctylphosphine (TOP) were prepared following the methods pioneered by Murray et al.[22] QD radii are quoted from calibration curves based on the same authors' transmission electron microscopy and small-angle X-ray scattering results. All absorption spectra were obtained using a HP UV-vis spectrometer with 1-nm resolution in a 1-cm path length quartz cell. Dispersions of colloidal QDs were optically clear by eye, and the measured scattering was less than 0.1% of the incident light. Thus, for the rest of this article, we approximate C_{ext} as being equal to C_{abs}. For measurements of C_{abs} versus solvent refractive index, a concentration series of well-washed dispersions of QDs was prepared in five different solvents. Identical volumes of a concentrated QD dispersion in hexane were added to the new solvent (approximately 0.1% hexane by volume in the final solution). The extinction coefficient in each solvent was deduced from the slope of the Beer's law plot.

For each sample in the size series, the QD absorption cross section was determined as follows: a known number of moles of precursors (n_{Cd}) were used to prepare the QDs, with dimethyl cadmium being the limiting reagent. A small fraction of QDs was then isolated from the original known volume of growth solution. The typical size dispersion in this fractionated sample was ~5%. Assuming a 100% reaction yield, the concentration of particles is equal to the concentration of cadmium divided by the number of cadmium atoms per particle ($N_{Cd/QD}$), where

$$N_{Cd/QD} = \frac{4}{3}\pi a^3 \frac{2}{V_{unit}} \tag{5}$$

a is the radius of the QD, and V_{unit} is the volume of the unit cell containing two CdSe units. The bulk CdSe wurtzite unit cell volume is 112 Å^3. Powder X-ray diffraction studies of CdSe QDs have shown less than 0.5% lattice contraction compared to the bulk parameters.[22]

The integrated areas of the absorption spectra of the growth and the fractionated solutions were compared to obtain the relative concentration of QDs. The concentration of CdSe QDs in the size-selected fraction is given by

$$[QD] = \frac{\int_{350}^{700} A_{cut}(\lambda)\, d\lambda}{\int_{350}^{700} A_{growth}(\lambda)\, d\lambda} \frac{n_{Cd} Y}{V_{growth}} \frac{1}{N_{Cd/QD}} \tag{6}$$

where $A(\lambda)$ is the absorbance as a function of wavelength, Y is the reaction yield, and V_{growth} is the volume of the growth solution. The validity of this procedure is examined below. The reaction yield as a function of size is determined using thermal gravimetric analysis (TGA). For a separate set of samples having a narrow size distribution in the growth solution, the entire reaction preparation was precipitated, washed thoroughly with methanol to remove excess TOPO, and dried before performing the TGA.

Dilute dispersions are used for optical measurements; typically, both the growth and fractionated spectra are obtained from dispersions that have been diluted by a factor of 100. Once the concentration of QDs is known, the extinction coefficient is calculated using Beer's law, $\epsilon_\lambda = A_\lambda/cl$, where c is the concentration of chromophores (M) and l is the path length (cm). The extinction coefficient (M^{-1} cm^{-1}) is converted to a per particle absorption cross section (cm^2) using

$$C_{abs} = \frac{2303\epsilon_\lambda}{N_A} \tag{7}$$

where N_A is Avogadro's number.

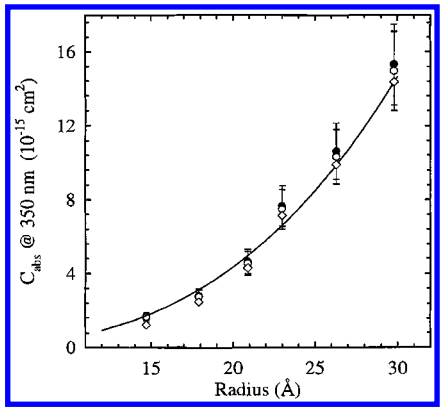

Figure 1. Observed and theoretical absorption cross section as a function of size for CdSe QDs dispersed in hexane. (◇) indicates C_{abs} based on the integrated absorption spectra; (●) indicates C_{abs} based on the integrated absorption spectra and corrected for the reaction yield as a function of size; and (○) indicates C_{abs} determined using the absorbances of the growth and fractionated solutions at 350 nm that were corrected for the reaction yield. The solid line is the theoretical curve calculated using eqs 2 and 3 and the literature parameters given in the text.

TABLE 1: Estimated Reaction Yield Based on Thermal Gravimetric Analysis

λ_{max} $1S_e1S_{3/2h}$	radius (Å)	wt % loss 25−600 °C	total yield (g)	inorganic yield (g)	% yield
498	13.9	23.9%	0.46	0.35	65.8%
526	16.8	18.5%	0.57	0.46	87.2%
600	25.9	12.0%	0.58	0.51	95.9%

IV. Results

The size-dependent absorption cross section at 350 nm determined using the procedure described in the previous section is plotted in Figure 1 both with (●) and without (◇) correcting the data for the absolute reaction yield. The reaction yield for each size was estimated by fitting the data in Table 1 to the function $y = a(1 - be^{-cx})$. The uncertainty in the data resulting from the radial size dispersion of the QDs (~5%) is indicated by the error bars. Surprisingly good agreement is observed with the theoretical curve that was calculated using eqs 2 and 3 and the complex refractive index for bulk CdSe[22,23] at 350 nm, which is $m_1 = 2.772 - 0.7726i$. We find that C_{abs} (cm^2) = $(5.501 \times 10^5)a^3$, where the particle radius a is in cm. The corresponding extinction coefficient ϵ_λ (M^{-1} cm^{-1}) = $(1.438 \times 10^{26})a^3$, again where the particle radius is in cm.

Figure 1 also shows that the relative concentrations of the growth and fractionated solutions may be simply estimated from the ratio of the absorbances at 350 nm (○). The integration method and the single point method for determining the concentration of QDs give the same results within experimental uncertainty, which indicates that the density of states is approximately constant at 350 nm and the absorbance is indicative of the number of unit cells present rather than the oscillator strength of a particular electronic transition.

In eq 6, it is implicitly assumed that the integrated oscillator strength (per unit cell) is constant even as the transition probabilities are redistributed among different electronic transi-

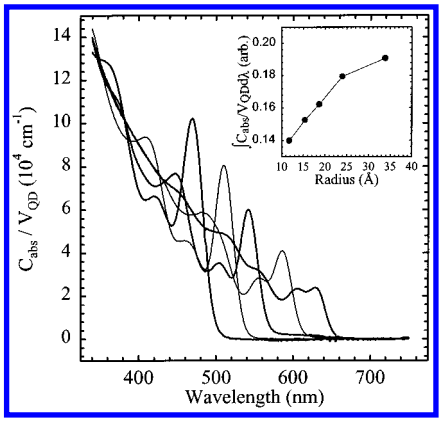

Figure 2. Room-temperature absorption cross section per CdSe unit versus wavelength for CdSe QDs dispersed in hexane. Each spectrum is divided by the volume of the QD to give the absorption cross section per CdSe unit. From right to left, spectra are shown for QDs with radii of 33.9, 24.0, 18.7, 15.4, and 11.8 Å . The inset shows the integrated area per unit volume as a function of the QD radius.

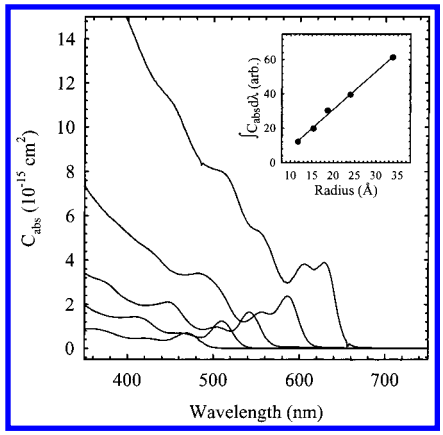

Figure 3. Room-temperature absorption cross section per QD for CdSe QDs dispersed in hexane. From right to left, spectra are shown for QDs with radii of 33.9 , 24.0, 18.7, 15.4, and 11.8 Å. In the inset, the integrated oscillator strength per particle for the lowest-energy transition ($1S_e1S_{3/2h}$) is plotted versus particle radius.

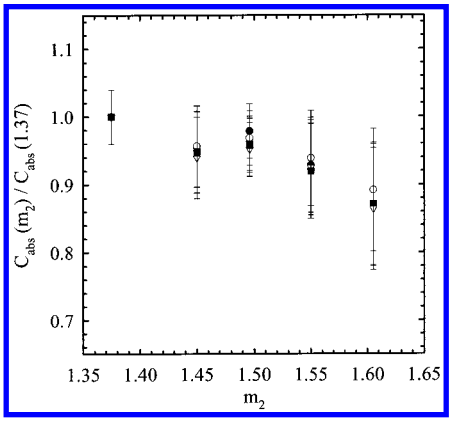

Figure 4. Effect of solvent refractive index on C_{abs} per QD for 24.0-Å CdSe QDs. The observed absorption cross section is plotted relative to C_{abs} for QDs in hexane at (●) 350, (○) 400, (▲) 457, (▽) 516, and (■) 553 nm. Error bars indicate the uncertainty in the measurement based on multiple runs.

tions as the QD size changes. Whereas ideally one would integrate over the full absorption band, this is not possible for QDs dispersed in most common solvents because the solvent absorption begins to dominate at UV wavelengths. To determine how much error is introduced by integrating only from 750 to 350 nm, a series of absorption spectra are plotted where each spectrum has been divided by the size-dependent C_{abs} (determined using the data in Figure 1) and by the QD volume to give the effective absorption cross section *per* CdSe unit (Figure 2). Plotted in the inset of Figure 2 is the size-dependent oscillator strength, integrated from 350 to 750 nm, per CdSe unit. Over this limited energy range, the total oscillator strength per CdSe unit varies weakly with QD radius. Thus, as long as the average QD radii in the growth and size-selected fractions are not significantly different, comparison of the total area under the absorption curve gives a good estimation of the relative concentrations.

The utility of having a well-known absorption cross section immediately becomes apparent as we examine the size-dependent oscillator strength of other transitions close to the band edge. Figure 2 clearly shows that as the QD radius is decreased the oscillator strength per CdSe unit of the lowest-energy transition ($1S_e1S_{3/2h}$)[25] increases and the spectra converge for wavelengths less than 400 nm. In the strong confinement regime where the particle radius is less than the Bohr exciton radius, within the effective mass approximation and neglecting Coulomb interactions, the $1S_e1S_{3/2h}$ oscillator strength per CdSe unit scales as $1/a^3$ because of the increased overlap of the electron and hole wave functions.[12−14] Because the particle volume is proportional to a^3, the oscillator strength of the $1S_e1S_{3/2h}$ transition *per* particle is therefore expected to be approximately constant. The shortcomings of this simple model are evident in Figure 3, where the $1S_e1S_{3/2h}$ integrated oscillator strength per particle is shown to grow approximately linearly with radius over this size range.

According to eqs 4a and b, the absorption cross section should increase with increasing solvent refractive index. The solvent dependence of the absorption cross section is examined in Figure 4 for various features in the linear spectrum. No changes in the intensity of electronic transitions were observed for transitions either high in the band or near the band edge. Instead, a slight downward trend in the absorption coefficient is observed throughout the band with increasing refractive index. The absorbance depended linearly on concentration for all of the solvents tested. Addition of capping ligands to the solutions made no difference within the instrumental reproducibility.

V. Discussion

Remarkably good agreement between the experimental data and theory is observed for the QDs dispersed in hexane. The success of the simple scattering theory suggests that the density of states for the QDs can be modeled as a continuum for absorption high in the band. Strong absorption bands for halogenated solvents that start below 375 nm complicate the interpretation of absorption data in solvents other than hexane. Near a strong absorption band, anomalous dispersion is expected, and the complex refractive index of the solvent should be used in calculations. Whereas these problems could be avoided by going to longer wavelengths, near the absorption edge for the QDs the polarizability clearly cannot be modeled using bulk CdSe parameters, and the effect of the discrete electronic states must be taken into account. The slight downward trend in the absorption coefficient with increasing refractive index was observed throughout the QD absorption spectrum (Figure 4).

One possible explanation for the insensitivity of the absorption cross section to the solvent refractive index could be the low refractive index ligand shell surrounding each QD. To model the effect of the ligand shell, it is straightforward to extend eq

4b to a sphere covered with a shell of a different material. The polarizability of a spherical core−shell structure embedded in a dielectric medium in a uniform electric field is

$$\epsilon = \epsilon_1(\omega) \qquad \text{for } 0 < r < a$$

$$\epsilon = \epsilon_2 \qquad \text{for } a < r < b$$

$$\epsilon = \epsilon_3 \qquad \text{for } r > b$$

$$f(\omega) = \frac{-9\epsilon_3\epsilon_2 b^3}{2a^3(\epsilon_2 - \epsilon_1(\omega))(\epsilon_2 - \epsilon_3) - b^3(\epsilon_1(\omega) + 2\epsilon_2)(\epsilon_2 + 2\epsilon_3)} \quad (8)$$

Equation 8 reduces to eq 4b for $a = b$ or $\epsilon_1 = \epsilon_2$ (in each case, ϵ is approximated by m^2).

Calculations show that inclusion of a low refractive index ligand shell does make the theoretical absorption cross section somewhat less sensitive to the refractive index of the medium. However, this phenomenon alone cannot account for the observations in Figure 4. The good agreement between the theory and the data for QDs in hexane may be explained by the fact that hexane and the TOPO/TOP ligands have similar dielectric constants. Pending more detailed modeling of the absorption cross section near the band edge, we suggest caution when using these results for QDs dispersed in media with dielectric constants that differ greatly from that of the capping ligand.

Finally, a condition for applying the scattering equations is that the mutual distances between the particles must be large compared to the size of the particles and large compared to the wavelength of light in the medium. In the Lorentz−Lorenz regime, it is assumed that the mutual distances of the particles are small compared to the wavelength of light ($a \ll \lambda$) and that the electric field to which a particle is exposed is due to the scattered fields of a large number of other molecules on all sides.[21] For a dilute dispersion of 20 Å QDs in hexane with a concentration of $\sim 2 \times 10^{-7}$ M ($A = 0.2$ at 350 nm), the average distance between particles (r) is $\sim$ 200 nm. Therefore, for visible excitation, r/λ is $\sim$1, and formally, the conditions for neither the Lorentz−Lorenz regime nor the scattering regime are satisfied. However, no deviation from the linear dependence on concentration has been observed for concentrated QD dispersions. As the particle concentration approaches that of close-packed QDs, significant deviations are expected, and the extinction coefficient should approach that of the bulk semiconductor.

VI. Conclusions

Excellent agreement between the measured and theoretical absorption cross sections for interband transitions far above the band edge for QDs in hexane is observed. The absorption cross section appears to be insensitive to the refractive index of the medium for common organic solvents. However, caution should be exercised when using these results for QDs dispersed in media with dielectric constants that differ greatly from that of the capping ligand until the issue of the screening from the ligand shell can be addressed. In addition, the simple theory suggests that significant deviations from Beer's law will be observed at particle concentrations approaching those of close-packed QD solids.

Acknowledgment. We thank V. Klimov and A. L. Efros for stimulating discussions and the NSF-funded MIT Harrison Spectroscopy Laboratory for support and for the use of its facilities. This research was funded in part through the NSF Materials Research Science and Engineering Center program and by the Office of Naval Research.

References and Notes

(1) Murray, C.; Kagan, C.; Bawendi, M. *Annu. Rev. Mater. Sci.* **2000**, *30*, 546−610.
(2) Efros, A.; Rosen, M. *Annu. Rev. Mater. Sci.* **2000**, *30*, 475−521.
(3) Woggon, U. *Optical Properties of Semiconductor Quantum Dots*; Springer: New York, 1997.
(4) Brus, L. *Appl. Phys. A: Mater. Sci. Process.* **1991**, *53*, 465−474.
(5) Bruchez, M.; Moronne, M.; Gin, P.; Weiss, S.; Alivisatos, A. P. *Science (Washington, D.C.)* **1998**, *281*, 2013−2016.
(6) Chan, W.; Nie, S. *Science (Washington, D.C.)* **1998**, *281*, 2016−2018.
(7) Mattoussi, H.; Mauro, J.; Goldman, E.; Anderson, G.; Sundar, V.; Mikulec, F.; Bawendi, M. *J. Am. Chem. Soc.* **2000**, *122*, 12142−12150.
(8) Vossmeyer, T.; Katsikas, L.; Giersig, M.; Popovic, I. G.; Diesner, K.; Chemseddine, A.; Eychmuller, A.; Weller, H. *J. Phys. Chem.* **1994**, *98*, 7665−7673.
(9) Shim, M.; Guyot-Sionnest, P. *J. Chem. Phys.* **1999**, *111*, 6955−6964.
(10) Schmelz, O.; Mews, A.; Basche, T.; Herrman, A.; Mullen, K. *Langmuir* **2001**, *17*, 2861−2865.
(11) Jacobsohn, M.; Banin, U. *J. Phys. Chem. B* **2000**, *104*, 1−5.
(12) Efros, A. L.; Efros, A. L. *Sov. Phys. Semiconductors* **1982**, *16*, 772−775.
(13) Brus, L. *J. Chem. Phys.* **1984**, *80*, 4403−4409.
(14) Kayanuma, Y. *Phys. Rev. B: Condens. Matter* **1988**, *38*, 9797−9805.
(15) Efros, A. L. *Superlattices Microstruct.* **1992**, *11*, 167−169.
(16) Ricard, D.; Ghanassi, M.; Schanne-Klein, M. C. *Opt. Commun.* **1994**, *108*, 311−318.
(17) Keller, O.; Garm, T. *Phys. Rev. B: Condens. Matter* **1995**, *52*, 4670−4673.
(18) Keller, O. *Phys. Rep.* **1996**, *268*, 85−262.
(19) Todorovic, G.; Milanovic, V.; Ikonic, Z.; Indjin, D. *Solid State Phenom.* **1998**, *61−62*, 235−238.
(20) Iwamatsu, M. *Jpn. J. Appl. Phys.* **1998**, *37*, 5620−5621.
(21) van de Hulst, H. C. *Light Scattering by Small Particles*, 2nd ed.; Dover Publications: New York, 1981.
(22) Murray, C. B.; Norris, D. J.; Bawendi, M. G. *J. Am. Chem. Soc.* **1993**, *115*, 8706−8715.
(23) *Handbook of Optical Constants II*; Palik, E. D., Ed.; Academic Press: Boston, 1991; Vol. 2.
(24) Ninomiya, S.; Adachi, S. *J. Appl. Phys.* **1995**, *78*, 4681−4689.
(25) For a detailed description of the electronic transitions that make up the linear optical absorption spectrum of CdSe QDs, see Norris, D. J.; Bawendi, M. G. *Phys. Rev. B* **1996**, *53*,16388.